

1. Introduction:

An interferometer has proven to be a very powerful diagnostic tool used in the diverse fields of science and engineering. We use a Michaelson interferometer to characterize the coherence behavior of our laser. In this interferometer, the laser from a single beam is split into two separate beams and recombined to study their coherence behavior by collecting the combined light either using a photo-detector or a camera. We use this behavior to judge the performance of different lasers for use in our system.

2. Interferometer setup - version one:

The coherence is the capacity of the light to interfere. The coherence length becomes essential for the application that requires the speckle contrast measurements. Equivalently, narrower the linewidth of the lasers width, better will be the contrast.

In order to primarily characterize the laser, the Michaelson interferometer is devised as shown in the Figure (1)

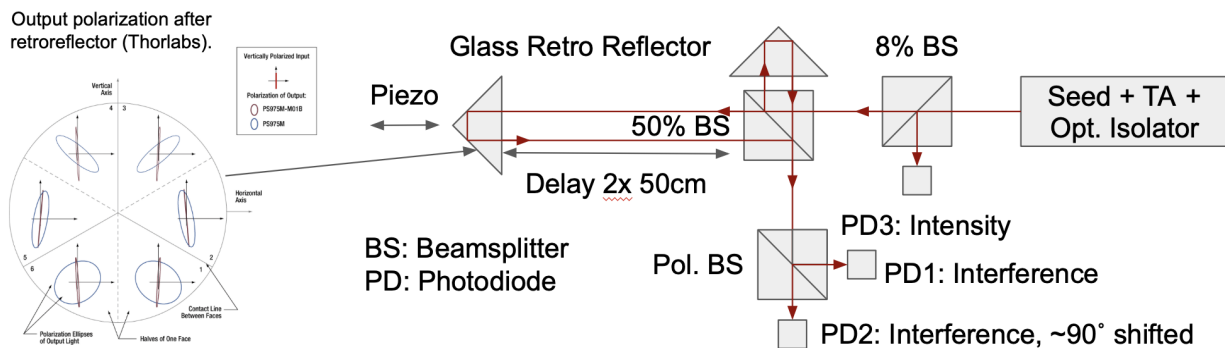



Figure 1

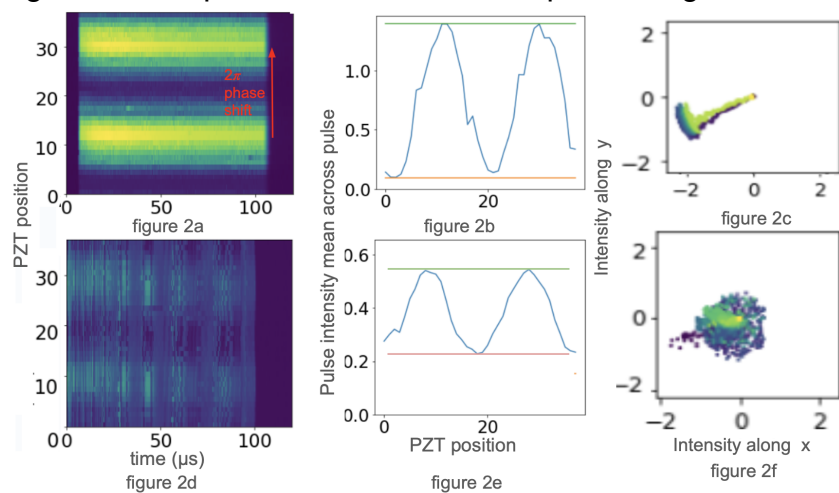
The Figure1 shows the original home built interferometer setup for the characterization of the laser, The PD3 monitors the intensity, the PD1 and PD2 collect the interferometer signal in two orthogonal directions to monitor the phase noise.

The output of the tapered amplifier (TA) and optical isolator is split using (8/92) beam splitter cube (BS). The 8% beam is aligned to the photodetector (PD3) to monitor the

	Engineering Study		Doc #:	D####
			Rev:	##
	Laser characterization using interferometer		Page:	2 of 10

intensity of the laser and 92% of the beam is coupled into the interferometer. The beam is then further split into two beams with a second non-polarizing beam splitter cube 50/50 (BS). One of the beams is retro-reflected at a shorter, fixed distance while the other is reflected at a longer, adjustable delay with a glass retro-reflector mounted onto the piezo-stage. The delay is set to ~ 100 cm in the longer arm of the interferometer. It is then combined with the reflected beam from the shorter, fixed arm. The combined beam is then further split into two orthogonal beams via polarizing beam splitter cube (PBS) and they are aligned to the photodetectors (PD1 and PD2) as shown in the Figure 1 to obtain the phase information along with the coherence behavior of the laser.

The typical interferometer signals and the phasor diagrams with the TA driven at a current of 5A with pulse width of 100 μ s are shown in Figure 2 for the comparison between good and underperforming TAs. A well performing TA shows smooth variation in the interference as we sweep the position of piezo (PZT) and the phase noise is tightly scattered compared to the underperforming TA. A poorly performing TA shows broader scattering of the phase noise and the interference pattern is also washed out. Figure 2b and 2e depict the mean interferometer signal across the pulse. The interferometer contrast is significantly reduced for the underperforming laser shown in Figure 2e compared to that of the well-performing laser in Figure 2b.



The Figure 2a and 2d show the interferometer signals collected at different PZT positions for good and bad lasers respectively. The Figure 2b and 2e are the intensity mean per pulse as a function of the PZT position and the Figure 2c and Figure 2f show the sample of phase variation during the laser pulse for single PZT position.

3. Simplified Michelson interferometer setup:

The hardware (optical elements, optomechanical and controller) used to build the simplified version of Michelson interferometer is shown in Figure 3. These are available in Thorlabs with the path number shown below each component. The test setup is shown in Figure 4.



Figure 3

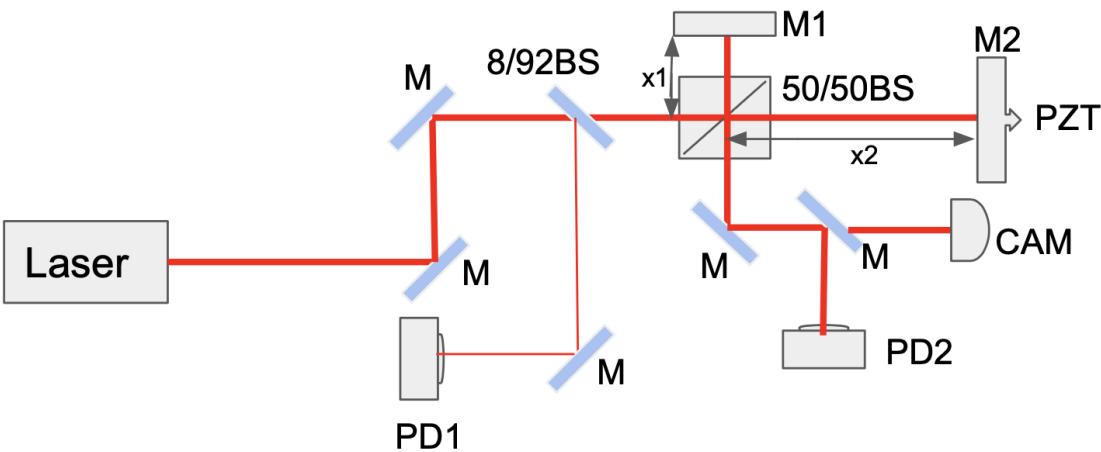


Figure 4

Figure 3 displays the major components used to build the interferometer and the instruments used to drive PZT, and monitor and collect the interferometer signals. Figure 4 shows the simplified Michelson interferometer setup.

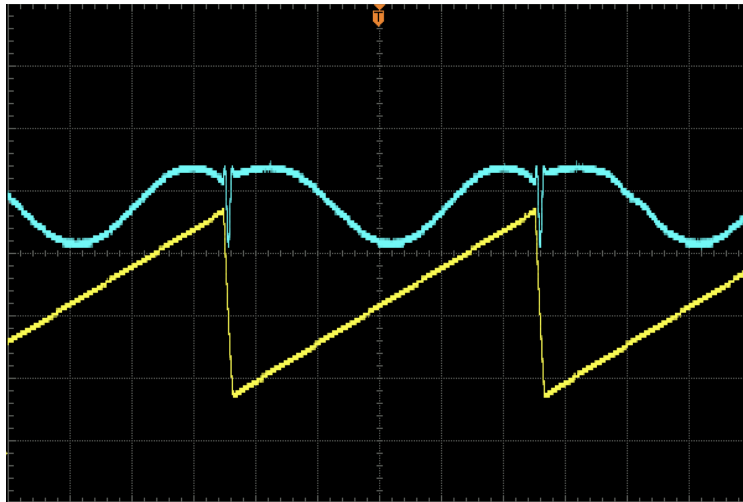


Figure 5a

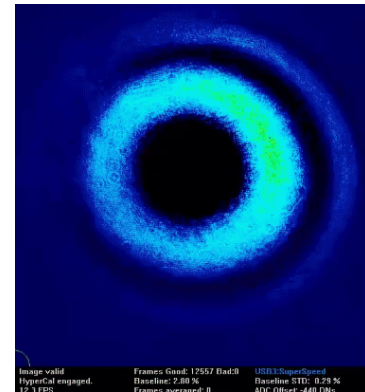


Figure 5b

In Figure 5a, the ramp applied to the PZT attached to the mirror on the adjustable arm of the interferometer is shown in yellow, the blue signal is the interferometer signal collected in the PD2 in Figure 4. Figure 5b shows the fringes captured in the camera CAM in Figure 4 during the ramp applied to the PZT.

4. Alignment and optimization of the interferometer:

- 4.1. Set the position of the adjustable arm of the interferometer.
- 4.2. Center the beams at the center of the mirrors M_1 and M_2 by adjusting two mirrors M and M after the laser.
- 4.3. Apply the ramp voltage to the PZT attached on the back of the mirror M_2 as shown in the yellow signal in Figure 5a.
- 4.4. Optimize the interferometer signal by tweaking the mirror M_2 to obtain an interferometer signal (blue) as shown in Figure 5a .
- 4.5. Alternatively, the camera can also be used to view the overlap of the two recombined beams. The Figure 5b is showing the fringe shifts corresponding to the ramp voltage applied to the PZT) (Note: The pattern of the fringe depends upon the alignments)

5. Calculation of the path difference:

The calculation of more accurate path difference is required for the estimation of full fringe shift (FFS), maxima to nearest maxima in order to determine the accurate chirping during the pulsing of the laser.

In order to determine the proper path difference we follow the procedure mentioned below.

- 5.1. Set the position of the adjustable arm-mirror mount with reference to the back edge of the base (x_{pos}) as shown in the Figure 7a,
- 5.2. Park the PZT voltage fixed to the max of the interferometer signal.
- 5.3. Note the wavelength on the wavelength meter (λ_1)
- 5.4. Slowly and continuously change the temperature of the laser/heat-sink until the interferometer level drops to minimum and returns to the same maximum level.
- 5.5. Note the wavelength on the wavelength meter (λ_2)
- 5.6. Repeat the steps 5a-5d for at least two more positions of the mirror.
- 5.7. The noted wavelength and the mirror mount edge positions are shown in table 1.

mirror mount edge position (cm)	λ -initial (nm)	λ -final (nm)	$\Delta\lambda$ (nm) measured	$\Delta\lambda$ (nm) simulated
420	935.8388	935.8261	0.0127	0.0135
370	935.8386	935.8328	0.0058	0.0053
320	935.8394	935.8361	0.0033	0.0033

table 1

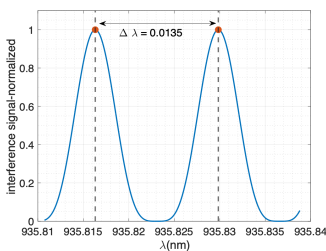


Figure 6a

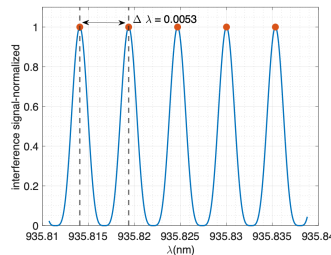


Figure 6b

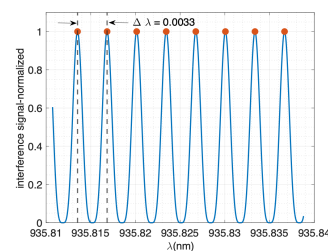


Figure 6c

The Figure 6a-6c shows the simulated full fringe shift (FFS) for the mirror mount edge positions of 420 mm, 370 mm and 320 mm respectively.

We define the path difference as

$$\text{path difference} = 2(x_2 - x_1)$$

Now using the relation between the path difference, wavelength and the change in wavelength. We get the plot in Figure 7b.

$$\text{path difference} = \frac{\lambda^2}{\Delta\lambda}$$

We can plot the data and fit it to a line and extrapolate the fitted line to the path-difference equals to 0. This intercept on the x axis provides the reference for the position of an adjustable arm mirror.

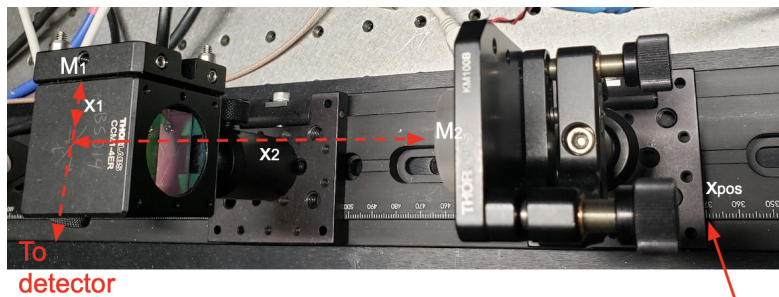


Figure 7a

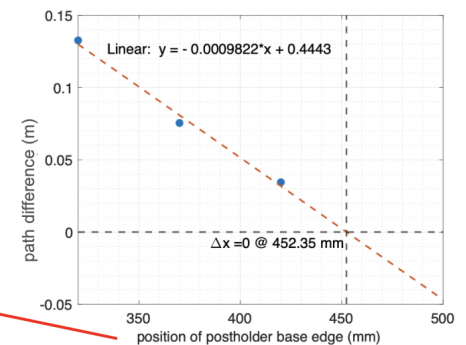


Figure 7b

Schematic of the beam paths in the two arms of the interferometer with the position of the mirrors shown as M_1 and M_2 . The exact positions of the mirrors are not known. Hence, we used the laser interference to measure the exact path difference as explained in section 5.

In our setup, the reference mirror mount edge positions for zero path difference corresponds to x_{pos} equals to ~ 452.35 mm.

$$\text{path difference} = 2(452.35 - \text{base edge position}) \times 10^{-3} \text{ m}$$

6. Calculation of full fringe shift (FFS) for the setup:

6.1. Once the proper path difference is determined. The position of the adjustable arm mirror mount base edge is set to multiple x-pos (Figure 7a)). The interferometer signals for path difference of 6.3cm and 26.3 cm are shown in the Figure 8a and 8b respectively.

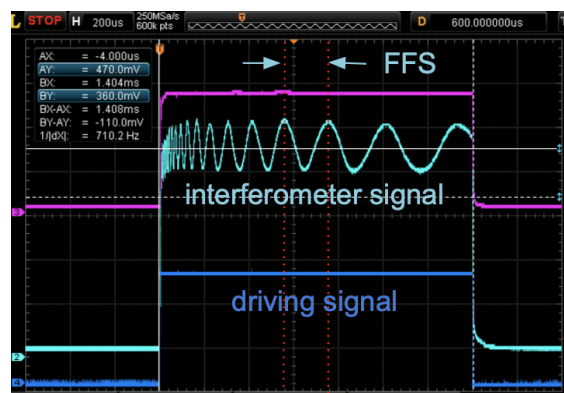


Figure 8a

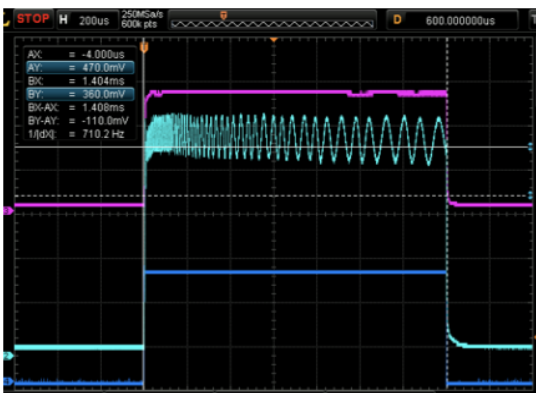


Figure 8b

Figure 8a and 8b show the interferometer signal (light blue), intensity (pink), driving current signal (dark blue) for the path difference of 6.3 cm and 26.3 cm respectively.

7. Measurement of the chirping of the lasers during pulse:

Finally, the mirror position is set to the base edge position x-pos equals to 40 cm equivalent to 82.47 cm of path difference.

The interferometer signal is collected and plotted as shown in Figure 9a. The data is smoothed and determines the peak positions. Each successive peak separation corresponds to full fringe shift (FFS). The number of peaks are counted and the approximate total chirping during the laser pulse is estimated as shown in the Figure 9b

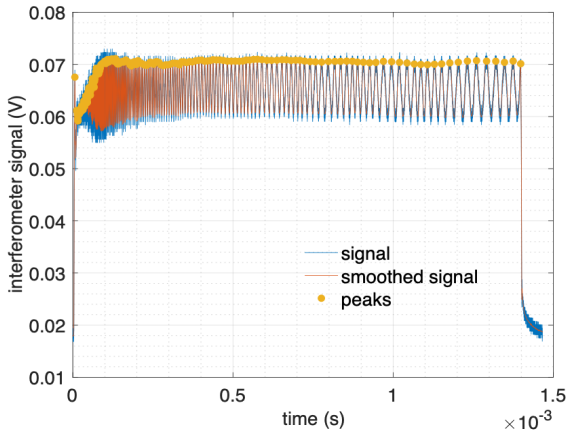


Figure 9a

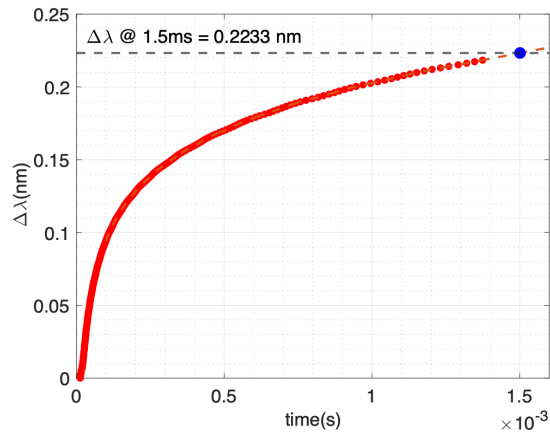


Figure 9b

Figure 9a shows the interferometer signal (light blue), smoothed signal (orange) and peak-position (yellow). Figure 9b is the plot of the chirping as a function of time.

8. Junction Temperature measurement:

The chirping in the laser can be caused due to the change in the driving current and the junction temperature. Since we are concerned about the chirping after 10 us of the beginning of the driving pulse, the driving current already reaches the stable region. Therefore, the chirping in the laser is caused due to the change in the junction temperature of the laser.

In order to measure the junction temperature, the LIV and wavelength data are collected for a set of fixed heat sink temperatures and a set of driving currents above threshold ensuring the thermal equilibrium has reached before each data collection [11.1].

The waste power is calculated from the data using the relation

$$P_j = I \times V - L$$

where P_j is the waste power, I , V and L are driving current, voltage and the output laser power respectively.

The corresponding measured wavelength is plotted against the calculated waste power. The data is fitted to a line and extrapolated, shown in Figure 10a. The intercept when the waste power is zero corresponds to the wavelength when the junction temperature T_j is equal to the heat sink temperature T_{hs} .

Now, using the wavelengths at the intercept for different heat sink temperatures a relation between them can be established as shown in the Figure 10b.

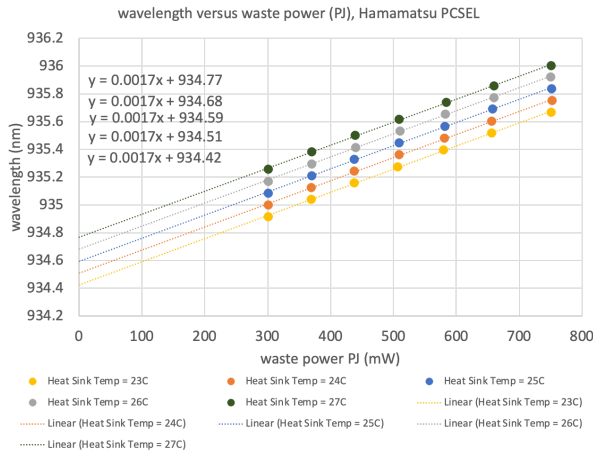


Figure 10a

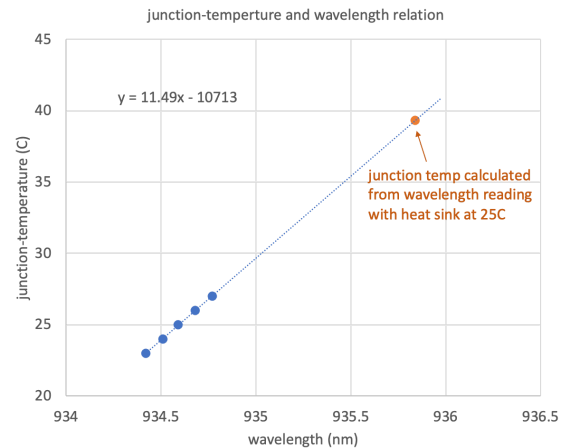


Figure 10b

Using the relation between T_j and wavelength of the laser

$$\Delta T_j = 11.49 \times \Delta \lambda = 2.56^\circ \text{C}$$

9. Conclusion:

The laser under test shows the chirping of $\Delta \lambda$ equals to ~ 0.223 nm corresponding to 77 GHz. This drift in the wavelength or frequency during the laser pulse corresponds to the change in temperature by 2.5C.


In our current system, the amount of acceptable chirping is ~ 65 MHz. Therefore, this particular laser is not acceptable for the speckle contrast measurement application due to the presence of the chirp washing out the speckle contrast.

10. Scripts:

The data result shown in Figure 9b is generated from the following [data](#) in Figure 9a with [scripts](#)

11. References:

- 11.1. ["Measuring high power laser diode junction temperature and package thermal impedance. Lawrence A. Johnson and Andrew Teh"](#)

	Engineering Study		Doc #:	D####
			Rev:	##
	Laser characterization using interferometer		Page:	10 of 10